Title

Functional Cellular Anti-Tumor Mechanisms are Augmented by Genetic Proteoglycan Targeting

Journal

Neoplasia, 22(2)

ISSN

1522-8002

Authors

Gupta, Purva
Johns, Scott C
Kim, So Young
et al.

Publication Date

2020-02-01

DOI

10.1016/j.neo.2019.11.003

Peer reviewed

NEOPLASIA
www.neoplasia.com

Volume 22 Number 2 February 2020 pp. 86–97

Original Research

Functional Cellular Anti-Tumor Mechanisms are Augmented by Genetic Proteoglycan Targeting

Purva Gupta [a,b]; Scott C. Johns [a,b]; So Young Kim [a,b]; Roland El Ghazal [b]; Elina I. Zuniga [c]; Mark M. Fuster [a,b,d,*]

[a] VA San Diego Healthcare System, Medical and Research Sections, La Jolla, CA 92161, United States; [b] Department of Medicine, Division of Pulmonary and Critical Care, University of California San Diego, La Jolla, CA 92037, United States; [c] Division of Biological Sciences, United States; [d] Glycobiology Research and Training Center, University of California San Diego, La Jolla, CA 92093, United States

Abstract

While recent research points to the importance of glycans in cancer immunity, knowledge on functional mechanisms is lacking. In lung carcinoma among other tumors, anti-tumor immunity is suppressed; and while some recent therapies boost T-cell mediated immunity by targeting immune-checkpoint pathways, robust responses are uncommon. Augmenting tumor antigen-specific immune responses by endogenous dendritic cells (DCs) is appealing from a specificity standpoint, but challenging. Here, we show that restricting a heparan sulfate (HS) loss-of-function mutation in the HS sulfating enzyme Ndst1 to predominantly conventional DCs (*Ndst1*f/f *CD11cCre*+ mutation) results in marked inhibition of Lewis lung carcinoma growth along with increased tumor-associated CD8+ T cells. In mice deficient in a major DC HS proteoglycan (syndecan-4), splenic CD8+ T cells showed increased anti-tumor cytotoxic responses relative to controls. Studies examining *Ndst1*f/f *CD11cCre* + mutants revealed that mutation was associated with an increase in anti-tumor cytolysis using either splenic CD8+ T cells or tumor-infiltrating (TIL) CD8+ T cells purified ex-vivo, and tested in pooled effector-to-target cytolytic assays against tumor cells from respective animals. On glycan compositional analysis, HS purified from *Ndst1*f/f *CD11cCre* + mutant DCs had reduced overall sulfation, including reduced sulfation of a tri-sulfated disaccharide species that was intriguingly abundant on wildtype DC HS. Interestingly, antigen presentation in the context of major histocompatibility complex class-I (MHC-I) was enhanced in mutant DCs, with more striking effects in the setting of HS under-sulfation, pointing to a likely regulatory role by sulfated glycans at the antigen/MHC-I – T-cell interface; and possibly future opportunities to improve antigen-specific T cell responses by immunologic targeting of HS proteoglycans in cancer.

Neoplasia (2019) xx xxx–xxx

Introduction

In cancer, dendritic cells (DCs) are typically subverted and inefficient in their classic functions as both professional antigen presenting cells and mediators of innate and adaptive immunity against novel (pathogen and/or tumor) stimuli. Classical DCs are able to respond to both immunostimulatory signals such as granulocyte–macrophage colony stimulatory factor (GM-CSF), interleukin-1 (IL-1), or interferon-gamma (IFNγ) [1–3], and pathogen associated toll-like receptor (TLR) signals (e.g., lipopolysaccharide (LPS), poly-IC or CpG motifs) [4] in a manner that promotes both

Abbreviations: BMDCs, Bone marrow dendritic cells, CD11c, CD11c locus, DC, Dendritic cell, HS, Heparan sulfate, HSPG, Heparan sulfate proteoglycan, LLC, Lewis lung carcinoma, LPS, Lipopolysaccharide, LysM, M Lysozyme locus, MHC, Major histocompatibility complex, Ndst, N-deacetylase/N-sulfotransferase, Ova, O-valbumin, Sdc, Syndecan, SIINFEKL, Ova peptide sequence for Ova_{257} Ova_{264}, TcR, T cell receptor, TIL, Tumor Infiltrating Lymphocyte, Treg, Regulatory T cell

* Address all correspondence to: Mark M. Fuster, MD, VA San Diego Healthcare System and UCSD Department of Medicine, Division of Pulmonary & Critical Care, 3350 La Jolla Village Drive, San Diego, CA 92161-111J, United States.
e-mail address: mfuster@ucsd.edu (M.M. Fuster), mfuster@ucsd.edu (M.M. Fuster).

https://doi.org/10.1016/j.neo.2019.11.003

maturation as well as characteristics needed for cellular immune-mediated clearance functions. The latter include increased performance in cross-presentation of antigen to T cells [5]. These responses are inhibited by a variety of immunosuppressive stimuli, including suppressive cytokines such as transforming growth factor-beta (TGF-β) and interleukin-10 (IL-10) or the presence of T-regulatory cells in the tumor microenvironment [3,6,7]. Moreover, while a variety of agents have been found to modulate co-stimulatory or co-inhibitory signals during DC – T cell interactions, improving the quality of the ``epicenter'' interaction between DC-presented antigen in the context of MHC and the T cell receptor remains an area of challenge and opportunity [8,9]. Harnessing this interaction positively may allow one to boost both the magnitude and the specificity of antigen-driven anti-tumor responses, and minimize non-specific immunologic activation and autoimmune side-effects during immunotherapy [10].

Previously, we had shown that reducing the sulfation of unique complex carbohydrates (specifically heparan sulfate) expressed by the lymphatic endothelium may affect chemokine-dependent trafficking of DCs toward lymphatic monolayers [11]. At the same time, we also questioned the immunologic effects of targeting glycans on the trafficking DC effector cells, with special interests in T cell responses and antigen presentation. Preliminary findings from targeting endogenous glycosaminoglycans on DCs revealed a slowing of lymphatic chemokine-driven DC trafficking, implying a role for DC cell-surface HS in DC migration kinetics; and promotion of DC maturation was also noted [12]. Moreover, moderate inhibition of tumor growth in mice was observed when genetic HS targeting was directed to myeloid-derived monocytes, consisting of DCs enriched in a mixture of macrophages and granulocytes that were likely targeted to some extent as well. While DCs purified from such tumors showed increased maturation, the myeloid mutation remained somewhat non-specific; and the functional effects of such genetic glycan alterations on DC glycan composition, anti-tumor DC-mediated immune functions (including CD8+ T cell proliferation and MHC associated antigen presentation) remain undiscovered.

In this work, we have restricted *Ndst1* mutation to CD11c+ cells *in vivo* to thereby achieve reduced sulfation of HS in predominantly conventional lymphoid-resident and migratory DCs (cDCs and mDCs) [13,14]. We herein demonstrate that driving such a mutation in this family of DCs results in a relatively more dramatic inhibitory effect on experimental tumor growth. Additionally, using a Lewis lung carcinoma model, we investigate and report the functional consequences of HS mutation on mechanisms of anti-tumor immunity, examining how under-sulfated HS on the DC surface results in improved ex-vivo CD8+ T cell mediated tumor cytolysis and boosts MHC-I associated antigen-presenting capacity. Moreover, similar outcomes are demonstrated in the setting of a loss-of-function mutation in a major DC-associated HS proteoglycan, syndecan-4. These insights on the increased magnitude of anti-tumor effects (with greater DC mutation specificity *in vivo*) paired with the functional importance of under-sulfated DC HS on antigen presentation and augmented functional CD8+ T cell anti-tumor immunity highlight novel biological mechanisms as well as a basis for therapeutic development.

Methods

Cell Lines and Cell Culture

Lewis Lung Carcinoma Cells (LL/2; ATCC) were cultured in DMEM Hi-glucose with 10% fetal bovine serum (FBS) and 1% penicillin/streptomycin. Cells were harvested using Accutase (Corning) after 5 min incubation and cell counting after neutralization. Primary cells in other studies included isolated tumor cells from subcutaneous tumors; CD8+ T cells from spleens or tumors; and DCs from bone marrow as described.

Primary Cell Preparations

All CD8+ T cells were prepared fresh. Spleen CD8+ T cells were prepared through mechanical spleen dissociation and passage through 40 μm filters followed by magnetic-column negative selection according to manufacturer instructions (Dynabeads Untouched CD8; Invitrogen). Tumor cells for cytolytic assays were prepared from subcutaneous tumors as follows: At day 14 following LLC subcutaneous inoculation, tumors were dissected from euthanized mice, rinsed with PBS, minced with a razor in a small petri-dish, and 5 ml of 0.2% Collagenase (Sigma) and 15 μg/ml DNase I (Sigma) solution was added, with digestion at 37 °C on a rotating platform for 1 h. Single-cell suspensions were obtained by filtering digests through 100 μm filters. Magnetic bead separation of tumor cells was performed through negative selection according to the tumor cell isolation kit manufacturer (Miltenyi, 130–110-187). For CD8+ T cells from tumors (TILs), filtered tumor digests were washed in labeling buffer (0.5% BSA, 2 mM EDTA in PBS), with the cell pellet resuspended to a concentration of 1.0×10^7 cells/ml, and incubated in 5 μg/ml biotinylated anti-CD8+ antibody (Life Technologies) at 4 °C for 1 h. Subsequent labeling with magnetic anti-biotin microbeads and positive selection was carried out according to the manufacturer (Miltenyi). Bone marrow dendritic cells (BMDCs) were prepared from femurs dissected from freshly euthanized mice using sterile technique: Marrow was washed from femurs using a 25 gauge needle/syringe with ice-cold serum free RPMI-1640 (Gibco) into a 15 ml conical tube. Cells were resuspended in DC growth medium [RPMI-1640 supplemented with penicillin/streptomycin (100 U/ml and 100 μg/ml, respectively; Sigma), L-glutamine (2 mM; Corning), beta-mercaptoethanol (55 μM; Gibco), 10% heat-inactivated FBS, 1 mM nonessential amino acids (Invitrogen), 10 mM HEPES (Affymetrix), and 20 ng/ml GM-CSF (Peprotech). Differentiation over 10 days was performed with media changes every 3 days.

Genetic Mouse Models

For targeting HS N-sulfation in conventional DCs, the *Cd11c* transgenic strain (B6.Cg-Tg(Itgax-cre)1-1Reiz/J #008068 JaxMice) [13] was crossed extensively onto mice with a conditional mutation in N-deacety lase/N-sulfotransferase-1 (*Ndst1* f/f) previously backcrossed onto C57Bl/6. This yielded *Ndst1*f/f *CD11cCre* + mutants, wherein *Cre*-mediated deletion of a loxP flanked segment of the *Ndst1* Exon-2 coding region was achieved under control of the CD11c integrin prompter/enhancer; with *Ndst1*f/f *CD11cCre*− littermates used as wildtype controls. For the *Ndst1*f/f *LysMCre* mutant line, targeting *Ndst1* mutation to the myeloid lineage, mice were generated and maintained as previously published [12]. *Syndecan4* knockout mice (*Sdc4*−/−) bear a constitutional deficiency in the HS proteoglycan syndecan-4 [15], and were originally a kind gift from Dr. Paul Goetinck. They were backcrossed onto C57Bl/6. The reduction in *Sdc4* expression in homozygous null mutants has previously been shown to be >99% by qPCR [12].

Mouse Tumors and Models

LLC cells were injected ($5.0x10^5$ cells in 100 μl serum-free DMEM) subcutaneously into the hindquarter of isoflorane-anesthetized mice. Tumors in *Ndst1*f/f *LysMCre* mutants and *Sdc4* mutants were grown simultaneously over 20 days with close observation and monitoring according to approved protocols, and mice euthanized using carbon dioxide according to American Veterinary Medical Association guidelines. Tumors were grown on the *Ndst1*f/f *CD11cCre* mutant background under similar conditions and observation protocol (over 14 d period). Tumors were extracted and handled in sterile manner; and measured by calipers with volume based on ellipsoid method [$0.5 \times \text{length} \times (\text{width})^2$]. Cell

preparations from tumors were carried out as described (see Primary cell preparations). For intra-tracheal short-term tumor establishment, culture-harvested LLC cells were instilled (1.0×10^6 cells in 100 µl PBS) by intra-tracheal intubation into isoflorane-anaesthetized mice using methods as published [16]. Mice were sacrificed after 1 week; and bronchiolar-alveolar lavage (BAL) fluid was collected by suture-securing a blunt-ended 19 gauge needle cannulated into the trachea with 1.5 ml total PBS injected (in three 0.5 ml BAL washes). Animal studies were approved by the local institutional animal-care-and-use-committee (IACUC).

Dendritic Cell Preparations from Tissues

Following tissue digests, magnetic separation of DCs (CD11c + cells) was carried out per manufacturer instructions: Cells were labeled with CD11c microBeads (Miltenyi), loaded onto MACS MS magnetic bead columns, and separated using a magnetic separator (Miltenyi MiniMACS) according to manufacturer protocol to collect CD11c+ cell populations. Quantitative PCR (as described separately) was used to assess *Ndst1* expression in positively selected cells.

Flow Cytometry

Dendritic Cell Maturation Assessments

For maturation markers, cells were labeled in 2 µg/ml of PE-labeled anti-CD86 antibody (Biolegend, 105007) and 2 µg/ml APC-labeled anti-MHC-II antibody (Life Technologies, 17–5321) for 1 h on ice; and following washing, acquisition was carried out on a Beckman Coulter Cytoflex cytometer. As a maturation control, *Ndst1*f/f *CD11cCre*+ and *Cre*− DCs were incubated with or without 1 µg/ml O55:B5 lipopolysaccharide (LPS) for 6 h at 37 °C. The cells were allowed to mature overnight prior to labeling for flow cytometry. *CD8+ T cell analyses:* Purified CD8+ T cells from spleen or tumor were analyzed for purity by labeling with 2 µg/ml of anti-mouse CD8α PE (Tonbo, 50–0081) followed by incubation for 1 h on ice. Unlabeled cells and isotype-matched secondary antibody were used as controls; with flow cytometry to determine %CD8+ T cells. *DC antigen presentation:* For model-antigen loading, SIINFEKL Ova peptide at 30 µM was incubated for 2 h with cells for each genotype. Washed cells were then incubated with CD16/32 (FC block) in FACS buffer, and resuspended in 100 µl flow buffer with either 2 µg/ml of anti-mouse SIINFEKL/H-2 Kb APC (mAb 25-D1.16; Life Technologies, 17-5743-80), isotype control antibody, or non-antibody containing medium; and labeling for 1 h on ice. (Antibody clone 25-D1.16 specifically detects SIINFEKL peptide in the context of MHC-I.) Washed cells were analyzed on the cytometer, with relative histogram shift in mean fluorescence intensity (MFI) as compared to control used to quantify level of antigen/MHC-I presentation for any given sample. Analysis of data was carried out using FlowJo (V X.0.7).

BAL CD8+ T-Cell Analysis

Initial net BAL cell concentration was determined; and FC-block was carried out for 15 min, and 2 µg/ml of anti-mouse CD8α PE (Tonobo, 50–0081) was incubated with cells for 1 h on ice. Unlabeled cells and isotype-match secondary antibody were used as controls; and flow cytometry was used to determine %CD8+ T cells in the total BAL population.

Cytolysis Assays and Cell Preparations

LLC cells isolated from subcutaneous tumors in *Ndst1*f/f *CD11cCre*+ mutant and *Cre*− control mice were mixed with CD8+ T-cells from spleens or tumors (at 10:1 and 20:1 CD8+ T cell to tumor cell Effector:Target ratios) following appropriate dilutions of cells from primary-cell preparations as described separately. Most experiments involved 1.0×10^5 CD8+ T cells mixed with 5.0×10^3 LLC tumor cells (i.e., for 20:1 ratio) in a final volume of 100 µl of DMEM medium. Cells were plated in triplicate for each experimental sample on a V-bottom 96-well plate. A media control was added for each experiment as background. The plate was incubated overnight at 37 °C to allow for cytolysis, and cytotoxicity was assayed using the CytoTox-Glo (Promega) kit according to manufacturer recommendations. Luminescence was read on a DTX Multimode Detector (Beckman Coulter) to detect luminescent protease-leak cytoxicity signals.

Real time Quantitative PCR (qPCR)

Total RNA was purified from cells with a RNAqueous 4-PCR kit (Ambion); and a SuperScript III kit (Invitrogen) was used to reverse-transcribe cDNA according to manufacturer instructions. Real-time PCR was carried out using an iQ Sybr Green Supermix Kit (BioRad) with 100 ng cDNA: Primer sequences (5′–3′) were as follows:

Ndst1 (forward 5′-GGACATCTGGTCTAAG-3′; reverse 5′-GATG CCTTTGTGATAG-3′),
Sdc1 (forward 5′-GGAGCAGGACTTCACCTTTG-3′; reverse 5′-T ACAGCATGAAACCCACCAG-3′),
Sdc2 (forward 5′-GCTGCTCCAAAAGTGGAAAC-3′; reverse 5′-C AGCAATGACAGCTGCTAGG-3′),
Sdc3 (forward 5′-GAGCCTGACATCCCTGAGAG-3′; reverse 5′-C CCACAGCTACCACCTCATT-3′),
Sdc4 (forward 5′-GAGCCCTACCAGACGATGAG-3′; reverse 5′-C AGTGCTGGACATTGACACC-3′).

PCR cycle conditions were as follows: 95 °C for 3 min followed by 40 cycles of 95 °C for 15 s, 59 °C for 45 s, and 72 °C for 45 s. Relative expression of a target gene was normalized against expression level of GAPDH or beta-Actin as indicated using the $2^{-\Delta\Delta Ct}$ method with ultimate expression as target mRNA as a percentage of GAPDH or beta-Actin expression [17].

Glycan Compositional Analysis

Purification of HS from BMDCs was carried out using HS preparation methods as previously described [18]. Cells were harvested from 10-day GM-CSF based DC differentiation cultures of marrow from the femurs of *Ndst1*f/f *CD11cCre*+ versus *Cre*− control mice as described for BMDC Primary Cell Preparations, above. Briefly, following glycan depolymerization with heparin lyases overnight, disaccharide analysis was carried out using quantitative liquid chromatography/mass spectrometry (LC/MS) [19]: After drying samples down, aniline labeling of disaccharide reducing ends was carried out (in 15 µl of 1 M $NaCNBH_3$ and $[^{12}C_6]$aniline freshly prepared in dimethyl sulfoxide/acetic acid (7:3, v/v) for 16 h at 37 °C) with products dried down. Using a C18 reversed phase column (0.21 × 15 cm; Thermo), derivatized disaccharides were separated with ion pairing agent (dibutylamine, Sigma) [20], and eluted ions of interest were monitored in negative ion mode on a mass spectrometer (LTQ Orbitrap, Thermo-Finnigan; capillary temp 150 °C; spray voltage 4.0 kV). Extracted ion current data were analyzed with Qual Browser software (Thermo-Finnigan). Quantitative composition analysis of disaccharides was performed by comparison with known amounts of differentially labeled standard $[^{13}C_6]$aniline added to the sample before LC/MS.

Western Blotting

Culture-differentiated DCs were exposed to O55:B5 LPS at 0.1 μg/ml for various time points. Cells were collected and centrifuged to pellets that were lysed in 100 μl 1X RIPA buffer (Teknova) supplemented with 1 mM Sodium orthovanadate, 1 mM PMSF and 10 μl/ml protease inhibitor cocktail and stored at −20 °C. Protein was quantified from thawed samples using a Micro BCA protein assay kit according to manufacturer protocol (Thermo) and Spectramax 190 microplate reader with concentrations calculated for equal loading. Samples were loaded onto a pre-cast 4%-15% gel (BIO-RAD) with a Precision Plus Protein Kaleidoscope ladder (BIO-RAD) and run at 180 V for 30 min in 1X Tris/Glycine/SDS buffer (BIO-RAD). Protein was transferred onto 0.2 μm Nitrocellulose filter paper sandwiches (BIO-RAD) in transfer buffer (100 mM CAPS and 20% methanol) at 30 V for 2 h in the cold. For phospho-NF-kB p65 subunit labeling, membranes were rinsed with 1X Tween-20/Tris-buffer saline (TTBS), and blocked for 1 h in Odyssey Blocking buffer (LI-COR). Phospho NF-kB p65 antibody (Cell Signaling, 3031 s) diluted in blocking buffer (1:1000) was incubated on the membrane at 4 °C on a shaker overnight. Membranes were washed 4X with 1X TTBS for 15 min; and IRDye 800CW goat anti-rabbit IgG secondary antibody diluted in blocking buffer (1:10,000) was used to incubate the membrane for 1 h at room temp in the dark, on a shaker. Washed membranes were air dried in the dark and scanned (LI-COR Odyssey) to detect bands with intensities calculated using Odyssey software.

Statistics

Mean values (þSD) were obtained for absolute and normalized tumor volumes, cytolysis determinations, tumor T-cell indices, BAL T cell percentages, and qPCR expression values. Comparisons of means were made by Student's T-test with the difference considered significant at $P < 0.05$. A one sample T-test was used for comparing changes in flow-cytometric mean fluorescence intensity (MFI) representing antigen presentation by mutant DCs (relative to normalized values of control DCs in individual experiments).

Results

Augmented Anti-Tumor DC Functions in Sdc4−/− Mice, and a Strategy to Enrich HS Targeting on DCs

We introduced glycan-targeted genetic models to examine roles of HS in tumor immunity, with a combined evaluation of Lewis lung carcinoma (LLC) tumor growth in two known models targeting HS on the DC cell surface. This was with an eye to ex-vivo mechanistic analyses using HS-deficient DCs. In first tumor models, we specifically employed published mouse models wherein we originally had begun to characterize maturation and trafficking properties of HS-deficient myelo-monocytic cells as well as tumor immunophenotyping on HS-deficient genetic backgrounds [12]. In extended tumor-growth studies in mice bearing (i) a myeloid-driven mutation in *Ndst1* (with under-sulfated HS chains on myeloid-derived monocytes/DCs and some macrophages/granulocytes [21]) and (ii) a systemic mutation in the HS proteoglycan core protein syndecan-4 (*Sdc4*) which is strongly expressed on DCs [12], we found: Moderate (in *Ndst1* mutant) and more marked (in *Sdc4* mutant) inhibition in tumor growth when the two mutations were examined simultaneously (Figure 1A). For initial ex-vivo mechanistic studies, given the magnitude of the tumor pheontype, we chose to examine the effect of mutation on the cytolytic properties of CD8 + splenocytes from tumor-bearing *Sdc4−/−* mice against harvested tumor cells from the respective mice. Mutation was associated with increased CD8+ T-cell mediated tumor cytolysis (Figure 1B). Given these findings and the importance of DC-mediated antigen presentation in the development of specific cytotoxic T cell responses, and since mutation could theoretically affect functional properties of both DCs and T cells in *Sdc4* mutants, we next examined whether *Sdc4* deficiency specifically on DCs purified from the mice might be associated with unique antigen presentation properties: Using an antibody that detects model antigen (Ova SIINFEKL) on antigen-pulsed DCs in the context of MHC-I (anti-SIINFEKL/H-2 Kb), and probing cultured bone marrow derived DCs (BMDCs) from *Sdc4−/−* mice versus wildtype controls with this antibody by flow cytometry revealed that mutation is associated with a significant increase in antigen presentation by the cultured DCs (Figure 1C).

Given the above findings and the possibility that HS deficiency (or altering the fine structure of HS) on DCs might augment mechanisms that boost anti-tumor cytolysis by CD8+ splenocytes at the end of a tumor growth period, including antigen presentation, we sought to increase the specificity of glycan targeting on DCs in vivo, while keeping robust representation across conventional DC lines. With this strategy and focus (Figure 1D), we generated *Ndst1*f/f *CD11cCre+* (and *Cre−* floxed wild-type control littermates), and assessed deletion efficiency in DCs isolated from distinct tissues, including organ-level deletion (lungs) as well as tumor-derived DCs (TIDCs) (Figure 1E). Since CD11c may be expressed to some extent in macrophages, we assessed BMDCs (used in several experiments herein) for presence of F4/80+ macrophages by flow cytometry (Figure 1F), wherein day-10 (standard differentiation period) GM-CSF differentiated cells from culture demonstrated up to 70% CD11c+ cells, with under 20% macrophages (CD11c+ F4/80+ cells) at time of harvest. This marrow preparation is thus enriched with a robust DC population for in vitro studies used herein for mechanistic studies using primary gene-targeted DCs. Upon establishing this new and more specific targeting strategy, we additionally examined how *Ndst1* mutation in the cultured primary DCs would affect syndecan-4 (or another syndecan) core protein expression in *Ndst1* mutant (*Cre+*) and wildtype control (*Cre-*) DCs from culture, and found no significant up-regulation of the two dominant syndecan core proteins (Sdc3 and Sdc4) expressed by *Ndst1*f/f *CD11cCre+* mutant DCs (Figure 1G). While Sdc1 appeared to be up-regulated in mutant cells, it was minimally expressed to begin with; and thus, mutation in DC *Ndst1* does not appear to lead to major HS chain up-regulation by key transmembrane (syndecan) HSPG species.

Tumor Phenotype of a CD11c Driven Mutation in HS Biosynthesis

Growth of LLC tumors in *Ndst1*f/f *CD11cCre+* mutants was markedly inhibited in comparison to that in floxed *Cre−* littermates (Figure 2A). Interestingly, the magnitude of experimental tumor inhibition on the *Ndst1*f/f *CD11cCre+* background is considerably greater than that which we found in tumor models in *Ndst1*f/f *LysMCre+* mutant mice (where mutation was targeted broadly to myeloid cells including DCs (with culture enrichment), macrophages and granulocytes [13,21], as in prior work [12]. Restricting mutation of *Ndst1* to the CD11c+ subset of monocytes (using *CD11cCre*) allows for more specific and robust enrichment of this mutation to a predominantly classic DC population [13,14]. This is also despite the fact that *Ndst1* deletion efficiency in tumor DCs isolated from the *CD11cCre* transgenic background (∼50% reduction by qPCR; Figure 1E), if anything, is modestly lower than that achieved in *LysMCre* mutant cells (∼70–80% reduction by qPCR) [12].

Beyond implying the unique importance of HS under-sulfation in this specific myeloid subset of monocytes in anti-tumor immunity (*Cre* expression in classic DCs > plasmacytoid DCs in this model [13]), we also find important in vivo effects of this mutation on tumor-associated CD8+ T cells. In particular, in addition to an increase in harvested CD8+ T cells from subcutaneous tumors on the *Ndst1*f/f/*CD11cCre+* background as compared to that of *Cre−* controls (Figure 2B); in a model of airway-

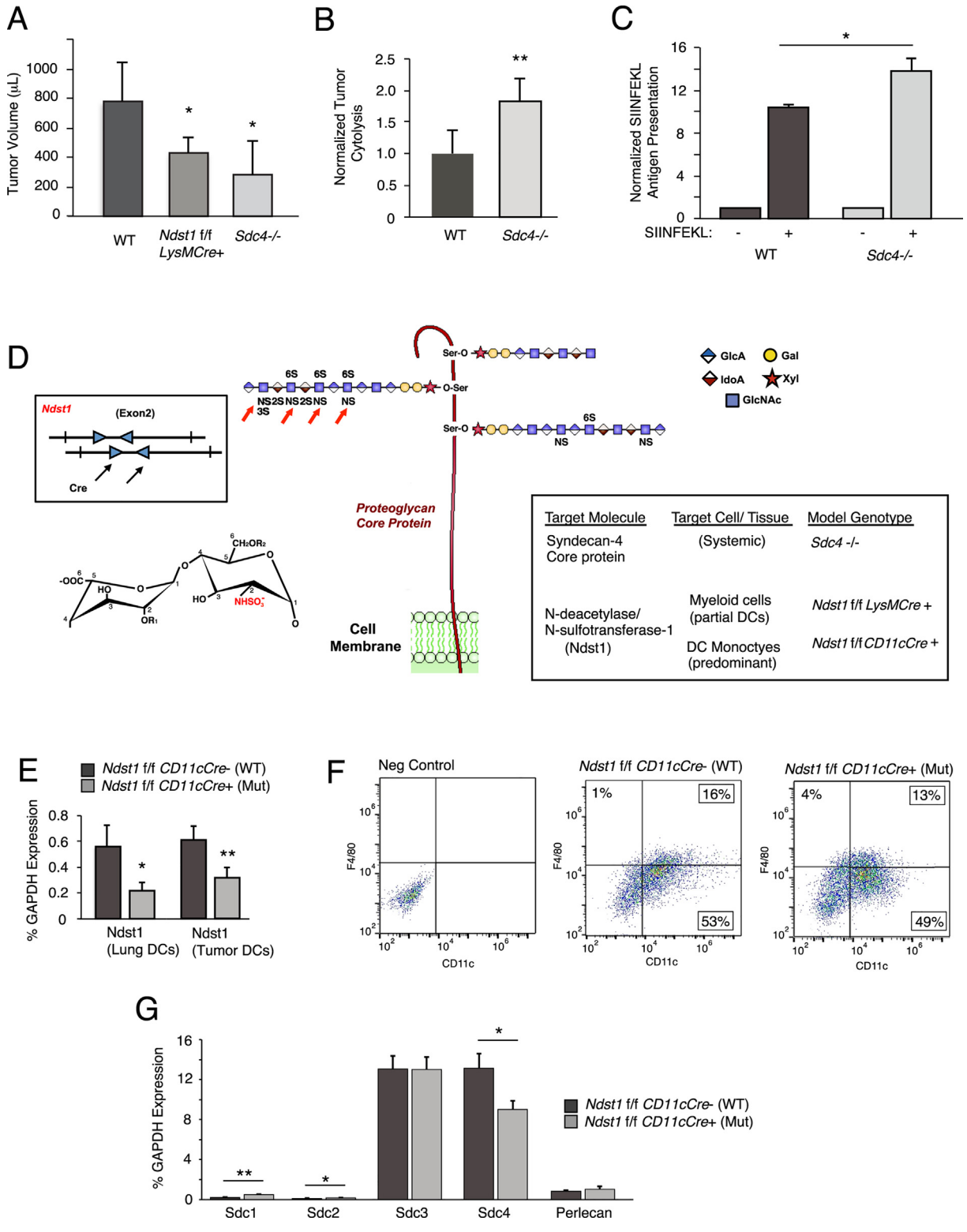

inoculated LLC tumor [22], we found increased CD8+ T cells in the bronchoalveolar lavage (BAL) of *Ndst1*f/f *CD11c*+ mutants as compared to that of *Cre*− controls (Figure 2D). This model was used to probe tumor-induced T cell proliferation in the lung through a relatively short-exposure model aimed to elicit an early cellular anti-tumor immune response in the lung as an orthotopic ``home'' for LLCs, and wherein lung-DC dependent T cell responses could be measured. More generally, the ability of DC *Ndst1* mutation to stimulate T cells in these experimental tumor assays demonstrates that DCs with under-sulfated HS appear to have augmented ability to stimulate T cell proliferation in vivo.

CD11cCre Driven Ndst1 Mutation: Analysis of HS Composition and Augmented DC Maturation

Isolation of a relatively large load of DCs from the pooled marrows of *Ndst1* f/f *CD11cCre*+ mutant versus *Cre*− wildtype mice (differentiated

Figure 1. Anti-tumor cellular immunity is increased in syndecan-4 deficient mice, and introduction of a genetic model to target glycan sulfation with optimum DC specificity. (A) Tumor growth of Lewis lung carcinomas (LLC) in the hindquarter of *Sdc4*−/− mice, *Ndst1*f/f *LysMCre*+ mutant mice bearing a myeloid-driven mutation in the major HS sulfating enzyme Ndst1, and *Cre*− wildtype (WT) controls was assessed at 20 days following subcutaneous inoculation of tumor cells in the hindquarter. Tumor volumes are graphed (**P* = 0.05 for difference in mean with WT; ***P* < 0.01 for difference in mean with WT). In separate anti-tumor cytolysis studies (B), we examined a model wherein ex-vivo CD8+ T-lymphocytes harvested from the spleen of a LLC tumor-bearing mouse are combined with tumor cells purified from a whole-tumor cell digest from the same mouse, and examined for cytolysis using a dead-cell protease release assay after overnight incubation at a 20:1 T-cell/Tumor-cell effector/target ratio. Graph shows the mean degree of anti-tumor cytolysis achieved by CD8+ T cells from *n* = 6 *Sdc4*−/− mice normalized to that of *n* = 5 WT C57Bl/6 control mice (***P* < 0.01 for difference). (C) Cultured bone marrow derived DCs from *Sdc4*−/− mutant and WT control mice were exposed to Ova SIINFEKL peptide, and examined for peptide presentation by flow cytometry using antibody that binds specifically to SIINFEKL in context of MHC-I. Graph shows-fold presentation of peptide-pulsed cells normalized to that of no-peptide controls run in parallel (**P* = 0.02 for difference). (D) Schematic introducing strategy to optimally target the sulfation fine structure of HS glycan chains on predominantly conventional DCs. Cartoon at center shows HS polymers tethered to HSPG core protein (i.e., syndecan-4 on membrane) through O-linkage to xylose, and with wildtype HS chain oriented to left of core protein modified by clustered sulfate domains initiated by the action of Ndst: NS, 2S, 6S, and 3S sulfate groups, where Ndst mediates NS modifications on glucosamine residues (red arrows). N-sulfation modification on a chemical HS disaccharide (uronic-acid and glucosamine residues) is shown to left (where -R1 and/or -R2 may be substituted with -H and/or -SO_3^-. Mice with a conditional mutation in *Ndst1* are crossed with CD11cCre transgenic mutants (box illustrates floxed/LoxP targets for Cre, arrows, in exon 2 of *Ndst1* gene) to target HS under-sulfation to DCs, (illustrated by under-sulfated HS chains oriented to right). (E) Reduced expression of *Ndst1* (qPCR, relative to GAPDH) in mutant DCs purified from lung (left histogram; from lungs of *n* = 3 mice per genotype; **P* = 0.03 for difference) and in DCs purified from LLC tumors (right; from tumors of *n* = 4 mice per genotype; ***P* < 0.01 for difference). (F) Flow cytometry of cultured marrow-derived mutant and control DCs showing CD11c+ F4/80-DC populations and CD11c+ F4/80+ macrophage populations (13% and 16% of cells in these preparations). (G) Expression of syndecan HSPG core proteins and the secreted HSPG perlecan (as %GAPDH) in DCs from *Ndst1*f/f *CD11cCre*+ mutant and *Cre*− control mice (**P* = 0.02 for *Sdc1* expression difference, ***P* < 0.01 for Sdc2 difference; **P* = 0.01 for Sdc4 difference).

over 10 days in culture under GM-CSF treatment and used in various in vitro functional studies) was required for simultaneous analyses of quantitative glycan sulfation and a confirmatory DC functional effect on maturation markers on the same cells. Glycosaminoglycan structural analysis of HS purified from mutant and wildtype DCs, through quantitative liquid chromatography/mass-spectrometry (LC/MS) of HS disaccharides released by heparin-lyase digestion of the purified HS, shows marked reductions in sulfation of HS disaccharides harvested from mutant DCs: In particular, DC-mutant HS had marked reductions in N-sulfated disaccharides, including mono (N-) sulfated and di-(2-O-, N-) (6-O-, N-) sulfated as well as more highly expressed unique tri-sulfated (N-, 2-O-, and 6-O-sulfated) moiety (Figure 3B). The latter appeared to be more abundant in relative quantity as a sulfated disaccharide species on DCs as compared, for example, to another key host cell-type from the mesenchymal compartment (e.g., lymphatic endothelium as analyzed in [23]). In addition, maturation analysis of the same cells by flow cytometry confirmed that the *Ndst1* mutation in marrow-derived DCs was associated with a marked increase in maturation markers, as assessed by the CD86/MHC-II dual-positive subset (Figure 3C); and with a further increase, as might be expected, following LPS stimulation as a known DC maturation stimulus. Curiously, NF-kB activation appears to be important for DC maturation [24]); and in pilot studies where we examined phosphorylation of the NF-kB subunit p65 to LPS stimulation in the same cells, while activation of control cells was somewhat variable, trends showed that for any given phospho-p65 response to LPS in *Ndst1*f/f *CD11cCre*− control DCs, responses by *Ndst1*f/f *CD11cCre*+ mutant cells were greater (Supplemental Figure 1).

The findings in studies on BMDCs are in the setting of a significant *Cre* mediated reduction in *Ndst1* expression in mutant marrow DCs (Figure 3A). The latter typically varied from 50% to 70% reductions in *Ndst1* expression, whether examining *CD11cCre* mediated *Ndst1* deletion efficiency in marrow derived (BM)DCs or in DCs purified (using anti-CD11c bead based methods) from the lung or LLC tumors (Figure 1E). Nevertheless, the genetic deletion efficiency was sufficient to drive relatively marked reductions in HS disaccharide sulfation (by LC/MS; Figure 3B) of HS disaccharides purified from GM-CSF differentiated BMDCs from the marrow of *Ndst1* f/f *CD11cCre*+ mutant mice. It should be noted that while GM-CSF differentiated marrow cells consisted of a major population of BMDCs, the degree to which a minor population of CD11c negative cells may have ``diluted'' the effects of mutation appears to be low, as the degree of reduction in the sulfation of HS from the cultured cells by compositional analysis (mean of 64% sulfation per HS disaccharide in HS from wildtype cells compared to mean of 37% sulfation per HS disaccharide from mutant cells; reported in Figure 3B legend) is of a similar order of magnitude as that of the overall degree of reduction in *Ndst1* expression by quantitative PCR analysis (Figure 3A) of mutant compared to wildtype cells from the same cultured preparations.

DC HS Under-Sulfation Augments Anti-Tumor CD8+ T Cell Activity and DC Antigen/MHC-I Presentation

Following experimental tumor establishment in *Ndst1*f/f *CD11cCre*+ mutants and *Cre*− littermates (as in Figure 2A), we functionally examined CD8+ T cells from spleens of mutant versus wildtype mice for degree of cytolytic anti-tumor responses, given both the tumor phenotype and increased DC maturation. Incubating CD8+ T-splenocytes harvested and pooled from tumor-bearing mice with LLC tumor cells purified and pooled from the same mice in an overnight Effector-to-Target exposure resulted in cytolytic responses that were augmented in the *Ndst1*f/f *CD11cCre*+ mutant background (Figure 4A). The difference in cytolysis relative to control was also greater at a higher CD8+ T-cell/Tumor-cell effector/target ratio. Since the *Ndst1*f/f *CD11cCre* genetic model uniquely targets DCs optimally, as a biologic proof-of-principle under these conditions (where T cells are genetically un-altered), we examined whether CD8 + T cells purified directly from the LLC tumors could exhibit similar augmented anti-tumor cytolytic behavior in the setting of the *Ndst1*f/f *CD11cCre*+ mutation; and indeed, this appeared to be the case (Figure 4B).

Mechanistically, we considered whether greater CD8+ T cell mediated cytolytic capacity in mutants (along with possibly greater DC maturation; Figure 3C) might be associated with differences in antigen presenting capacity by mutant DCs. Using BMDCs pulsed with the Ova peptide

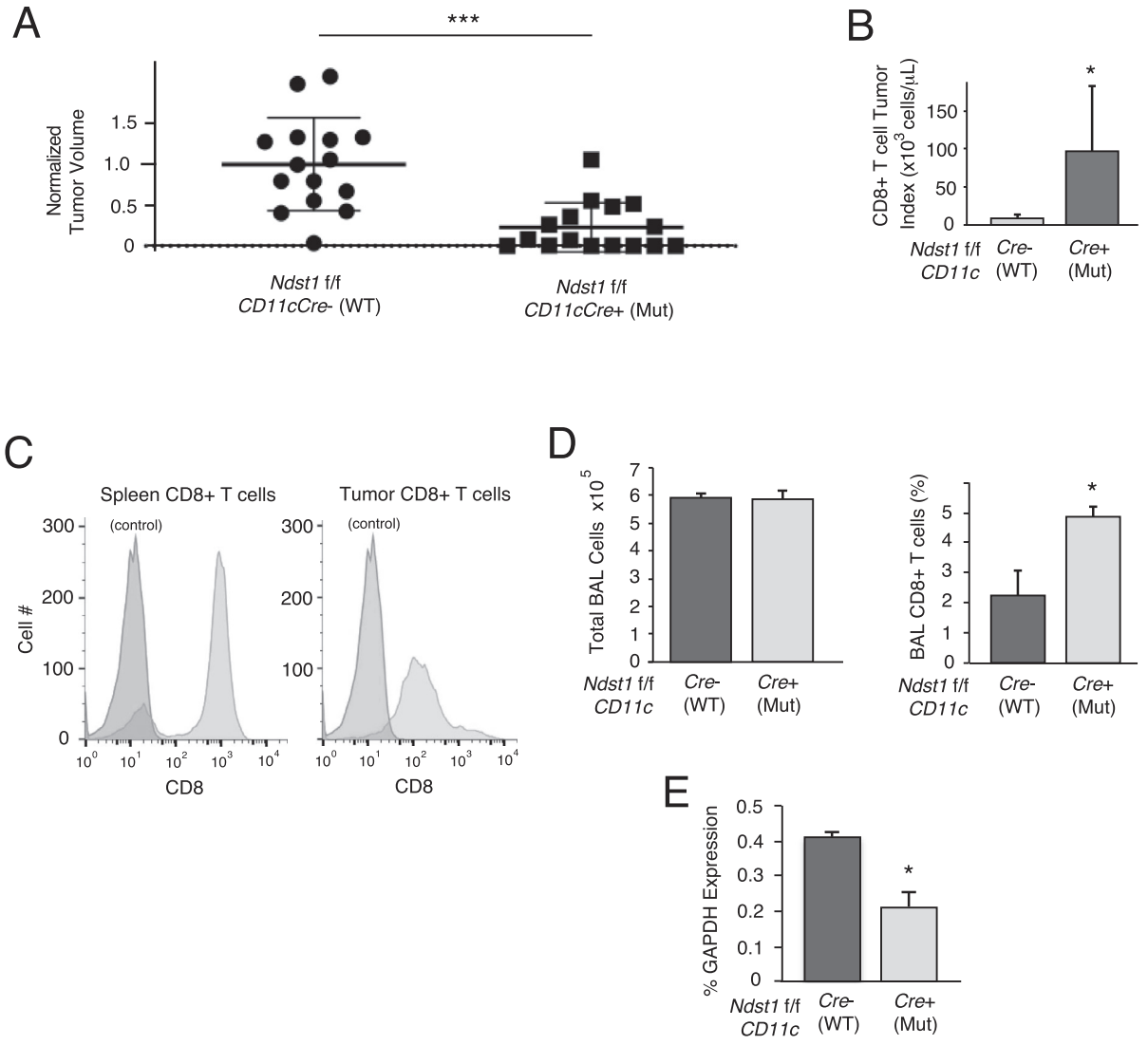

Figure 2. Tumor growth inhibition in *Ndst1*f/f *Cd11cCre* mutant mice and effects on tumor associated CD8+ T cell proliferation. (A) The volumes of LLC tumors grown in *Ndst1*f/f *Cd11cCre*+ mutants were compared to those of *Ndst1*f/f *CD11cCre*− control mice, measured 14 days after injection of LLC cells subcutaneously into the hindquarter. Scatter plot shows data from $n = 15$ controls versus $n = 16$ mutants normalized to the mean value for controls (***$P < 0.001$ for difference). (B) The CD8+ T cell index (number of CD8+ T cells per μL tumor volume) is shown for whole tumor digests from mutant versus wildtype control mice, showing mean indices for 6 separate experimental groups harvested from independent time periods; *$P < 0.05$ for difference. (C) Flow cytometric illustration of CD8+ T cells purified from tumor-digest purifications (using positive anti-CD8 bead selection method; right histogram), and from spleen-digest extractions (negative selection method; left histogram). (D) Bronchoalveolar lavage (BAL) total cell counts (left graph) and BAL CD8+ T cell counts (right graph) for BAL samples collected from $n = 3$ *Ndst1*f/f *Cd11cCre*+ mutants and $n = 3$ *Cre*− control mice at 7 days following intratracheal inoculation of LLC tumor cells; *$P < 0.05$ for difference in means. (E) Expression of *Ndst1* in DCs purified from cellular whole-lung digests of mice in (D), expressed as %GAPDH; *$P < 0.01$ for difference in means.

SIINFEKL (as used in Figure 1C in *Sdc4*−/− DC model-antigen studies) we found that DCs purified from *Ndst1*f/f *CD11cCre*+ mutants showed a marked increase in MHC/peptide on the DC surface relative to *Ndst1*f/f *CD11cCre*− controls (Figure 4C). Interestingly, we demonstrate that while *Sdc4* deletion results in a modest though significant increase in antigen presentation in SIINFEKL pulsed DCs (Figure 1C, showing ~30% increase in presentation among multiple Sdc4 mutant versus wildtype DC replicates), targeting the HS glycan broadly through under-sulfation (i.e., *Ndst1*f/f *CD11cCre*+ mutation) results in a markedly greater increase in antigen presentation as a result of the HS-chain specific mutation (comparing normalized increases in means under the two mutations in Figure 4C). An example of augmented antigen presentation in *Ndst1* mutant DCs is shown in Figure 4D. Original data examining effects of distinct (overnight versus 2 h) antigen pulsing periods for BMDCs using cells from which glycan analysis was carried out (Figure 3B) confirmed the effect of genotype on antigen presentation using those specific cells (shown in Supplemental Figure 2).

Discussion

In this study, we examine how restriction of a glycan mutation to a major subset of dendritic cells in vivo is sufficient to impact unique dendritic-cell specific mechanisms that augment anti-tumor T cell responses. By targeting mutation of a major HS sulfating enzyme (Ndst1)

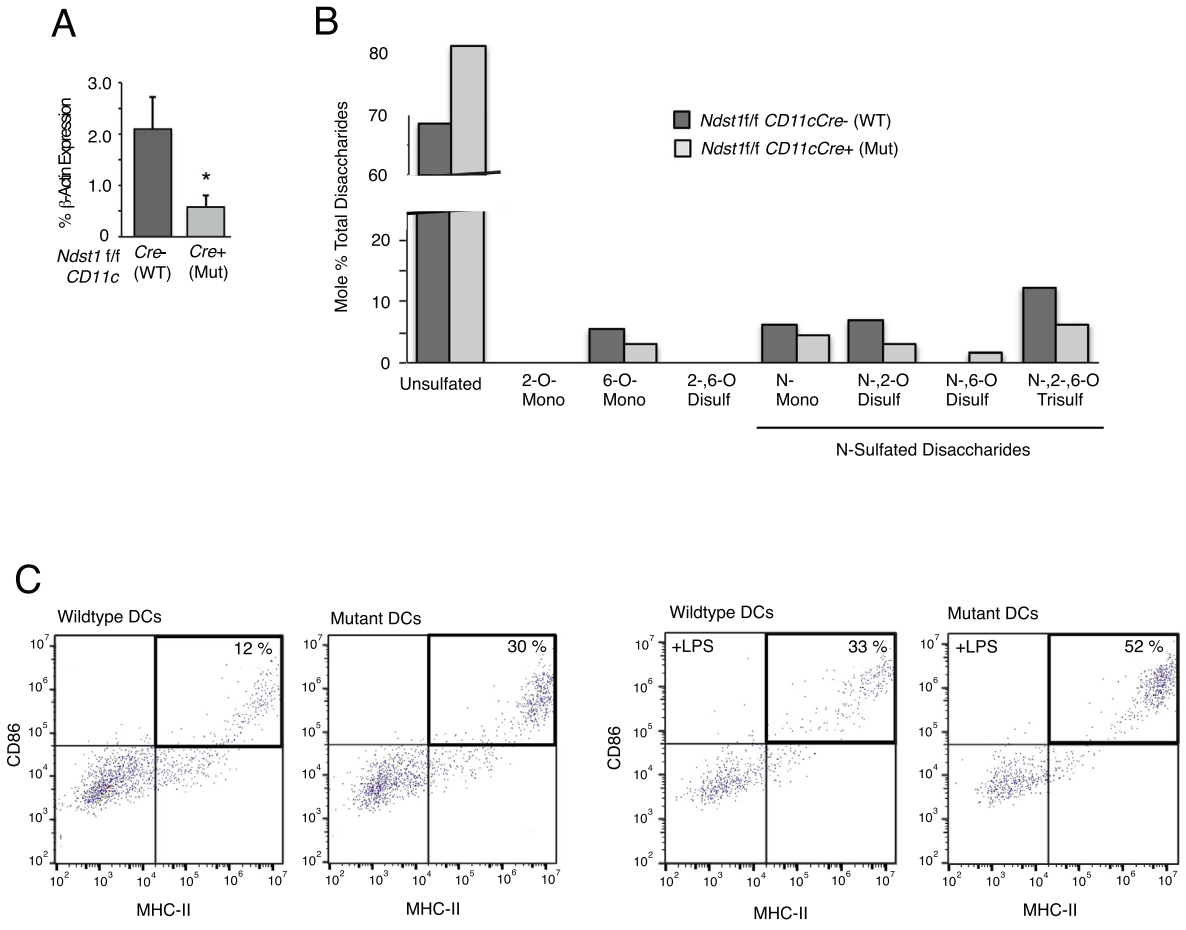

Figure 3. Glycan targeting and compositional analysis of HS purified from *Ndst1*f/f targeted DCs. (A) Deletion efficiency of *Ndst1* in day-10 differentiated cultured pooled BMDCs from *Ndst1*f/f *CD11cCre*+ versus *Cre*− control mice (run in triplicate per genotype); $^*P = 0.02$ for difference. (B) Sulfation of HS disaccharides (released from total heparin lyase digestion of HS) purified from *Ndst1*f/f *CD11cCre*+ versus *Cre*− control BMDCs was determined by liquid chromatography/mass spectrometry and quantified as a percentage of total disaccharides. Detected disaccharide species on graph are labeled below as unsulfated (68% for wildtype DCs versus 81% for mutant DCs) or as mono-, di-, and tri-sulfated species, with the latter being most abundant among sulfated species. The family of N-sulfated species is indicated, with the majority of N-sulfation reduced in mutant DCs. In general, *Ndst1* mutant HS also showed moderate reductions in 2-O and 6-O sulfation, which is consistent with the importance of Ndst1 in initiating HS sulfation domains on HS chains during biosynthesis. Overall, the average SO3 (sulfation) per disaccharide for *Ndst1* mutant HS was 37%, while the value for wildtype HS was 64%. (C) Maturation marker testing of cultured BMDCs isolated from mutants and littermate controls (corresponding to BMDCs shown in (B), differentiated in culture from pooled marrows of $n = 3$ mice per genotype). Cells were tested by flow cytometry for expression of standard markers of DC maturation (CD86 and MHC-II) in the absence or presence of LPS stimulation. For each harvested population, the percentage of dual-positive (CD86+/MHC-II+) cells is reported as the upper-right sub-population in dot plots corresponding to control versus mutant.

to cells that strongly express the integrin CD11c as the *Cre*-driving transgene (i.e., in *Ndst1*f/f *CD11cCre*+ mutants), we achieve under-sulfation of HS in vivo predominantly in conventional lymphoid-resident and migratory DCs (cDCs and mDCs) [13,14]. In association with a marked reduction in tumor growth on this mutant background, we find that the DC glycan mutation is also sufficient to augment ex-vivo cytolytic anti-tumor cell responses by CD8+ T-lymphocytes isolated from the spleens of tumor-bearing mutants. A particularly interesting feature of the mutation is that under-sulfation of HS on the DC surface appears to boost presentation of a DC molecular complex (antigen in the context of MHC-I) at the ``center'' of the immune synapse that drives antigen-mediated anti-tumor cytotoxic T cell responses. Similar anti-tumor DC-functional maturation associated events, including MHC-I/antigen modulation, are noted when we genetically reduce DC cell-surface HS through mutation in a major DC cell-surface HS proteoglycan (i.e., syndecan 4). These findings, wherein targeting an alteration in the fine-structure of HS to a major antigen-presenting DC subset results in augmented specific anti-tumor mechanisms, provide a basis for improving endogenous DC-mediated responses in cancer.

In prior studies we targeted mutation of *Ndst1* to myelo-monocytic cells [12], including DCs (but also some macrophages and neutrophils), through a *LysMCre* transgenic approach. This resulted in a modest though significant reduction in Lewis lung carcinoma (LLC) tumor growth; and we repeated tumor assessments in parallel to that in *Sdc4*−/− mutants upon initiating the mechanistic work herein (Figure 1A) to pair with our initial choice of mechanistic studies in *Sdc4*−/− mice. The latter mutation was associated with a somewhat more striking tumor growth inhibition phenotype (Figure 1A, right bar): So with this mutation in mind, we initially carried out a stringent functional anti-tumor immunity challenge, examining how the *Sdc4*−/− mutation might impact the ability

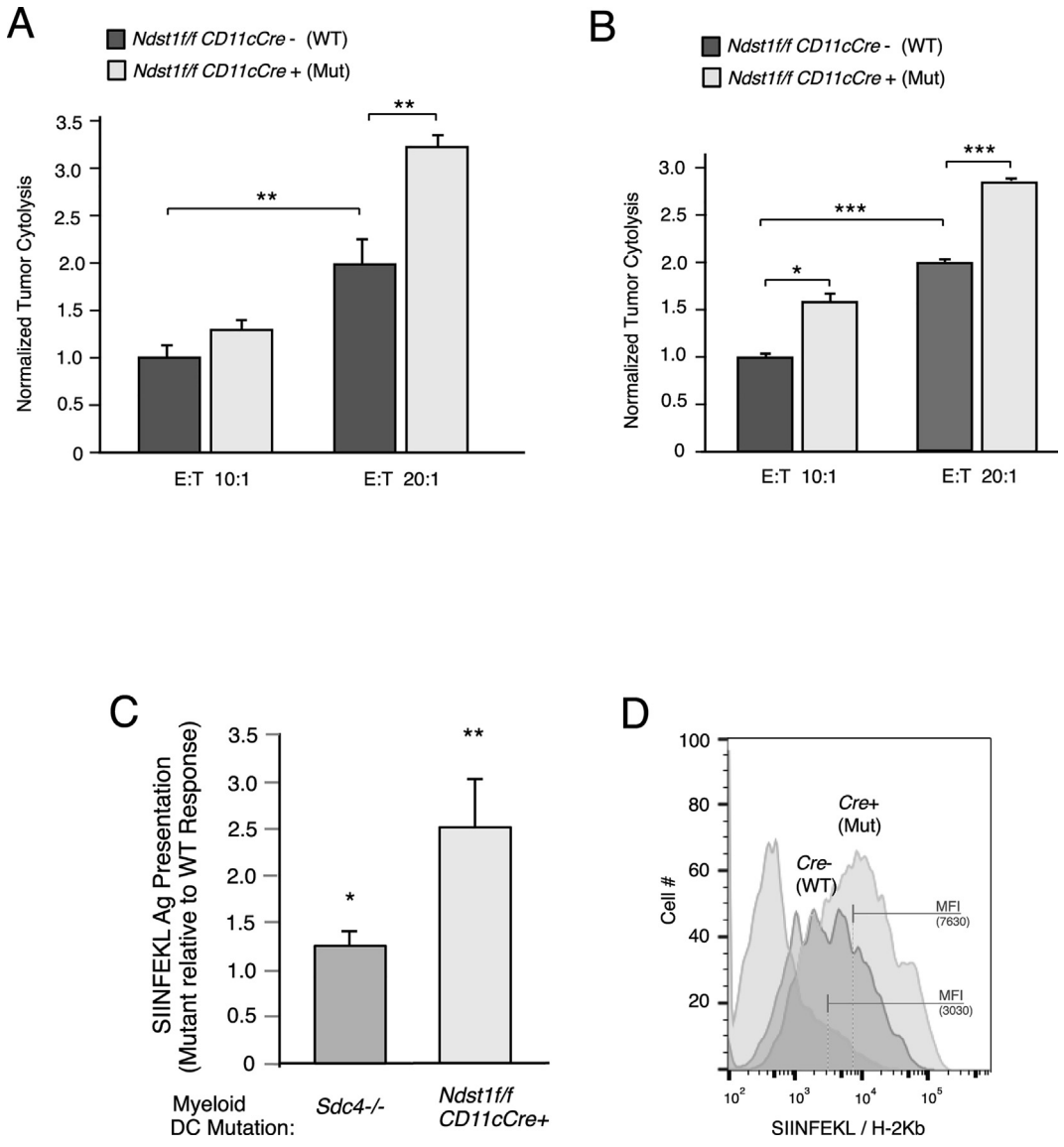

Figure 4. Functional CD8+ tumor-cytotoxic immunity and DC model antigen presentation are augmented in *Ndst1*f/f *CD11cCre* mutants. (A) Ex-vivo CD8+ T-lymphocytes harvested and pooled according to genotype from spleens of LLC tumor-bearing mice were combined with respective pooled purified tumor cells isolated from the same mice, and examined for cytolysis using a dead-cell protease release assay after overnight incubation at 10:1 and 20:1 T-Cell/Tumor-cell effector/target ratios. Graph for each condition shows the mean degree of anti-tumor cytolysis achieved by *Ndst1*f/f *CD11cCre*+ mutant versus *Ndst1*f/f *CD11cCre*− control CD8+ T cells normalized to that of controls; $P = 0.07$ for difference between means at 10:1 ratio; $^{**}P < 0.01$ for difference at 20:1 ratio; $^{**}P < 0.01$ for difference between wildtype controls at 10:1 versus 20:1. (B) Graph for cytolytic assays under 10:1 and 20:1 effector/target ratios using CD8+ T cells harvested directly from tumor digests as effector cells; $^{*}P = 0.01$ for difference between means at 10:1 ratio; $^{***}P < 0.001$ for difference at 20:1 ratio; $^{***}P < 0.001$ for difference between wildtype controls at 10:1 versus 20:1. (C) Cultured bone marrow derived DCs from *Ndst1*f/f *CD11cCre*+ mutant versus *Ndst1*f/f *CD11cCre*− control mice were exposed to Ova SIINFEKL peptide, and examined for peptide presentation by flow cytometry using antibody that binds specifically to SIINFEKL in context of MHC-I. Graph shows average increase in flow cytometric mean fluorescence intensity (MFI) representing specific SIINFEKL antigen presentation by mutant DCs relative to normalized values of control DCs in individual experiments (right bar; $^{*}P < 0.05$). To the left, bar is shown for response by Sdc4−/− mutant DCs relative to control for comparison (with reference to Figure 1C). (D) Representative flow cytometry histogram showing antigen presentation by SIINFEKL-pulsed *Ndst1*f/f *CD11cCre*+ mutant (right-most curve) versus *Ndst1*f/f *CD11cCre*− control DCs relative to baseline signal for non-pulsed control cells (left-most curve); MFI values indicated by bars on (log-scale) fluorescence axis.

of ex-vivo CD8+ T-splenocytes to generate direct anti-tumor cytolytic responses when incubated with tumor cells purified from the same respective mice. Importantly, CD8+ T cells from the spleens of *Sdc4*−/− mutant mice demonstrated greater cytolytic responses against their respective tumors than that for wildtype mice (Figure 1B). While the *Sdc4* mutation is systemic, DCs from the mutant animals are nevertheless deficient in HS (due to loss-of-function mutation in the syndecan-4 HSPG core protein), prompting us to hypothesize that HS deficiency on these cells might possibly boost the ability of the mutant DCs to activate anti-tumor T-cytotoxic responses through either nonspecific or even antigen-specific mechanisms. Considering the latter, we could test whether the HSPG (Sdc4) on the DC surface may serve to somehow regulate antigen pre-

sented on DCs, possibly in the context of MHC-I, wherein mutation may in some way facilitate presentation of antigen in the context of MHC-I. Indeed, in antigen presentation studies using an antibody that specifically binds model antigen (the Ova SIINFEKL peptide) in the context of MHC-I, we noted that DCs purified from *Sdc4*−/− mutant mice and pulsed with peptide demonstrated a significant (33%) increase in level of antigen presence (modeling presentation that might be sensed by a CD8+ T-cell receptor) on the DC surface by flow cytometry (Figure 1C).

With a focus on Ndst1 mutation, in early studies examining *Ndst1*f/f *LysMCre* mutants [12], we previously showed that cells with this mutation (targeted to a DC-enriched myelomonocytic population) are endowed with a phenotype characterized by slowed trafficking responses toward lymphatic chemokines and a cell-surface profile consistent with increased maturation. However, in vivo, it is unclear whether *Ndst1* deficiency in DCs dominates the anti-tumor response in the *Ndst1*f/f *LysMCre* LLC tumor model, where the effect of mutation on macrophages and granulocytes/neutrophils could theoretically also contribute. More importantly, beyond an anti-tumor immunophenotype with augmented maturation of purified DCs from the model, questions as to whether DC-specific anti-tumor mechanisms are glycan-modulated, their functional nature, and major downstream CD8+ T-cell responses have not been reported.

To address this, we first restricted the *Ndst1* mutation to CD11c expressing cells in the same in vivo models by generating *Ndst1*f/f *CD11cCre* mutants; and strikingly this resulted in a markedly more profound inhibition in tumor growth (Figure 2A), prompting us to examine basic DC mechanisms on this genetic background with optimal targeting of conventional DCs. Initially, we noted marked proliferative effects on tumor-associated CD8+ T cells: This appeared significant in both the subcutaneous tumor model (with direct measures of CD8+ T cells isolated from the tumors; Figure 2B) as well as an orthotopic lung model wherein distal-airway tumor inoculation (established via intra-tracheal LLC delivery) was associated with increased CD8+ T cells recovered in bronchoalveolar lavage (BAL) samples at time of experiment termination (Figure 2D). Tumor exposure in the latter model was limited to one week so as to activate an anti-tumor immunologic response toward the airway side of the alveolar-capillary barrier of the lung (rather than invasion of tumor deep into the lung parenchyma which might be achieved in longer-term models), hence driving lung CD8+ T cells toward the airway-inoculated tumor cells; and assayed/retrieved via BAL at termination of the short-term exposure. This served as an immunologic proof-of-concept to elicit lung T-cell responses in a short-term airway exposure model with LLC tumor cells. As a clinical extension, it is compelling to consider how DC-targeted *Ndst1* inhibition in human adenocarcinoma-in-situ (a common form of adenocarcinoma that spreads along airways and does not invade the alveolar epithelial basement membrane) might augment anti-tumor CD8+ T cell responses, and possibly inhibit growth and ultimate progressive basement membrane invasion by such tumors.

While proliferation of anti-tumor specific CD8+ T cells in vivo might result from hyper-mature DCs induced by this mutation (Figure 3C), it is also likely that an increase in antigen-driven specific functional T cell responses by the DC mutation serves to drive proliferative expansion of the anti-tumor CD8+ T cell population [9]. Since anti-tumor immunity during the 2-week model tumor growth period (referring to model in Figure 2A) may ultimately result in the ability of CD8+ T-splenocytes to exert an cytotoxic anti-tumor responses, the effect of a conventional DC-targeted *Ndst1* mutation (via the *CD11cCre* transgenic approach) on CD8+ T cell mediated cellular immunity was examined: We specifically examined how effectively CD8+ T cells pooled and purified from the spleens of tumor-bearing animals might lyse pooled tumor cells from the same animals in cytolytic effector:target studies wherein anti-tumor cytolytic effects could only be due to the DC-driven alteration in HS. We found an augmented capacity for cytolysis by such effector T cells from *Ndst1*f/f *CD11cCre*+ mutants (Figure 4A) as compared to that of *Cre*− controls; and while the findings corroborate data in the setting of *Sdc4*−/− mutation (as in Figure 1B) with partial absence of HS chains through mutation of a key DC HSPG, we highlight the specificity with regards to DC targeting in mechanistic studies using CD8+ T cells from *Ndst1*f/f *CD11cCre* mutants.

In further functional studies, augmented anti-tumor cytolytic effects by CD8+ T cells purified directly from tumors (reflecting the tumor-infiltrating ``TIL'' cells) on the *Ndst1*f/f *CD11cCre*+ mutant background (Figure 4B, as compared to that of *Cre*− controls) were paralleled by further mechanistic studies demonstrating an even greater effect of *Ndst1* mutation in augmenting SIINFEKL/MHC-I antigen presentation by purified DCs (Figure 4C, right bar with > 2-fold effect over control) when comparing to that achieved by *Sdc4*−/− mutant DCs (Figure 4C, left bar with ∼ 30% increase over control). The latter may be due to the fact that while the *Ndst1*f/f *CD11cCre*+ mutation is partial (Ndst1 deletion efficiency in DCs ∼ 50–70%), unlike Sdc4−/− mutation, glycan undersulfation via Ndst1 mutation affects all HSPGs, including Sdc3, Perlecan, or others (Figure 1G) that could conceivably contribute to antigen/MHC-I interactions with the TcR, or even the half-life of steric antigen display at the DC surface. The latter cell-biologic and biochemical mechanisms are beyond the scope of our functional mechanistic focus herein, but are worth consideration in future exploratory studies. Figure 5 shows a conceptual illustration indicating possible roles for HS chains tethered to HSPG core proteins on the DC surface, focused on regulatory interactions with antigen/MHC-I (where mutation or under-sulfation might augment antigen presentation for example) and/or other effects that directly or indirectly regulate maturation and DC functional outcomes when glycans are genetically targeted or modulated through other means.

The cytolytic studies herein provide a compelling mechanistic clue that this may be due to the anti-tumor immunologic effects of altering glycans on the surface of conventional DCs in the mouse models. Whether Sdc4 deficiency on the surface of T cells in *Sdc4*−/− mutants has additional effects is unknown; but it is curious that recent work has shown that Sdc4 on T cells may play a co-inhibitory role at the immune synapse through a T-cell inhibitory interaction with the DC (and myelomonocytic) ligand DC-HIL [25,26]. Thus, interference with Sdc4 (and possibly HS) expression may serve to increase CD8+ T cell immunity through novel mechanisms of increased antigen presentation proposed herein (i.e., referring to proof-of-principle as in Figure 4C), and possibly additionally through less ``antigen-specific'' immune-checkpoint pathways that may repress CD8+ T cell functions at baseline through expression of Sdc4 and/or HS on other proteoglycans. Interrogating these alternate systems may be helpful in the context of further therapeutic discovery studies, but lies beyond the scope of this work.

At a biochemical targeting level, as introduced above, the ability to achieve marked reductions in *Ndst1* was somewhat limited by the deletion efficiency of *CD11cCre* in tumor-derived DCs, lung-derived DCs (Figure 1E), and/or BMDCs (Figure 3A). Nevertheless, a strength is that we were able to confirm the effects of this degree of deletion efficiency on glycan composition through HS purification from mutant and wild-type BMDCs, followed by disaccharide analysis of HS disaccharide sulfation profiles by LC/MS. We believe that the HS composition analysis reflects that of predominantly BMDCs in the DC-enriched cultured marrow preparations. Macrophages in the GM-CSF differentiated marrow culture made up only a minority of the overall cell population (Figure 1F, upper right quadrants). Moreover, in a study by Gordts and colleagues examining HS compositional analysis of macrophages [27], including under *Ndst1* targeting, *Ndst1* mutation resulted in a very minimal (<10%) reduction in sulfation of HS (including the dominant trisulfated disaccharide species) from marrow-derived macrophages. In another study (not focused on targeting HS), the relative quantity of

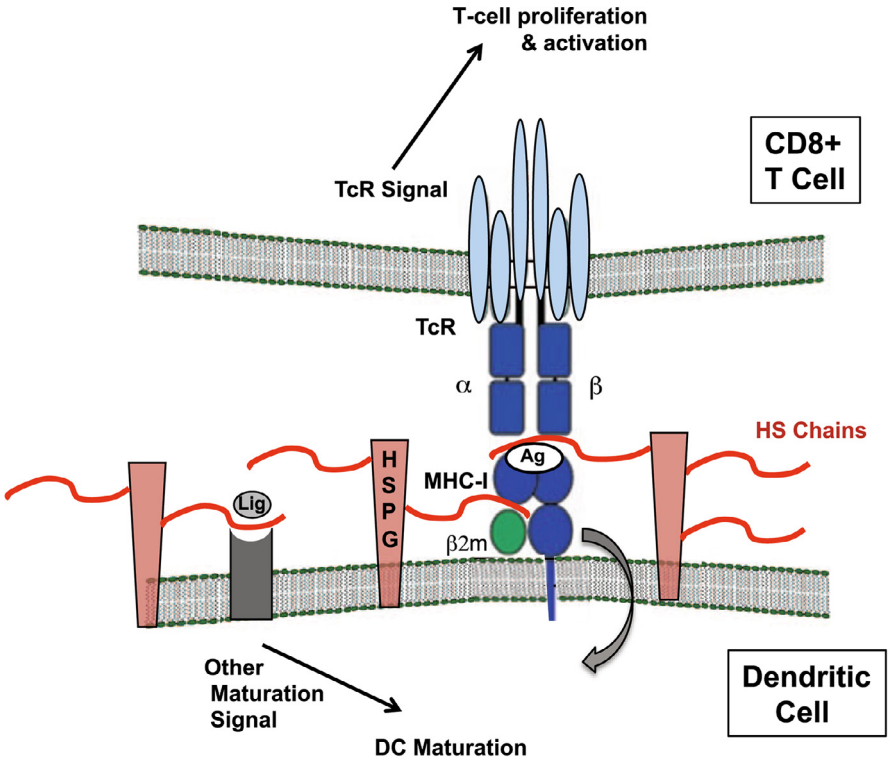

Figure 5. Model of DC – T cell interactions that may boost specific anti-tumor immunity in the setting of a targeted alteration in DC cell-surface HS glycan chains. Antigen presentation during a DC – T cell interaction is shown in the setting of HS proteoglycans with possible regulatory roles by HS chains. The DC (bottom) shows DC membrane with MHC-I (including β2-microglobulin, which is known to bind HS) and a bound antigen (Ag; which may represent a tumor antigen) interacting with a CD8+ T-cell receptor (TcR; top), wherein optimal presentation of Ag on MHC-I promotes TcR signal activation as well as T-cell proliferation. The possibility of control/internalization of Ag/MHC-I cell-surface complex on the DC surface (cell-inward curved arrow) by cell-surface HS proteoglycans (HSPGs; in pink with red HS chains) is illustrated. Altering HS chain sulfation may ``de-regulate'' and enhance quality and timing of the interaction. In addition, binding of toll-like-receptor (TLR) ligands (Lig) such as LPS to cognate receptors on the DC may also stimulate DC maturation: This may also be regulated by HS; and represented conceptually in diagram. Possible net effects of a DC-targeted HS chain mutation (i.e., under-sulfation through Ndst1 deficiency) may thus include: augmented quality of the Ag/MHC-I – TcR interaction, extended Ag presentation as a result of inhibited Ag/MHC-I internalization by HSPGs, and/or augmented TLR maturation responses.

the unique tri-sulfated HS disaccharide species (in both M1 and M2 monocyte-derived macrophages) was much more modest relative to that of other disaccharides [28]. With these data in mind, and with the minor contribution by macrophages in our preparations, we postulate that the marked difference in sulfated disaccharides between *Ndst1*-mutant and wildtype marrow-differentiated DC-enriched myeloid cells in our study must be due to major composition differences in a dominant DC population (including that of the dominant tri-sulfated disaccharide species).

While reductions in N-sulfation were achieved in mono-, di-, and trisulfated HS disaccharides, there were also reductions in 2-O-sulfation and 6-O-sulfation among the di- and tri-sulfated species: sulfation of these depends to some degree on N-sulfation of nascent HS chains during biosynthesis. Interestingly, the most abundant species was the most densely sulfated (trisulfated) species making up approximately 40% (molar %) of all sulfated disaccharides: In HS from *Ndst1* mutant DCs, under-sulfation was associated with approximately 50% reduction in this species (Figure 3B), indicating the importance of N-sulfation in the biosynthesis of this heavily sulfated species. It is curious as to why sulfation of HS on DCs may be so heavily represented by this densely-sulfated disaccharide (compare to HS composition from mesenchymal/endothelial cells for example). Whether this is somehow tied to DC immunologic function and regulatory control of antigen presentation by sulfated glycans is intriguing.

The findings herein have implications with respect to the possibility of harnessing novel therapeutic pathways to modulate DC function endogenously. The mechanistic findings are in line with goals to improve specific T-cell mediated anti-tumor immunity in a manner that may be responsive to a dynamic tumor-antigen landscape with possibilities for novel glycan targeting to boost antigen-specific CD8+ T cell immunity by endogenous DCs in the tumor and/or draining lymph nodes.

Acknowledgments

We thank Dr. J. Esko for advice and assistance with *Ndst1* f/f conditional mutant mice as well as Dr. Paul Goetinck for *Sdc4* homozygous null mutants. We appreciate assistance with glycan compositional analysis by Dr. Biswa Choudhury of the UCSD Glycotechnology Research and Training Center. We thank Dr. Z. Zhong and Dr. M. Karin for p65 signaling assistance.

Funding

Included the U.S. Department of Veterans Affairs Merit Review Program (VA Merit I01BX003688 to MMF), the American Lung Association (LCD-400697 to MMF), the Veterans Medical Research Foundation

(supporting MMF); and the National Institutes of Health (NIAID, R01 AI081923 to EIZ).

Appendix A. Supplementary data

Supplementary data to this article can be found online at https://doi.org/10.1016/j.neo.2019.11.003.

References

1. Pan J, Zhang M, Wang J, Wang Q, Xia D, Sun W, Zhang L, Yu H, Liu Y, Cao X. Interferon-gamma is an autocrine mediator for dendritic cell maturation. *Immunol Lett* 2004;**94**(1–2):141–51.
2. Wallet MA, Sen P, Tisch R. Immunoregulation of dendritic cells. *Clin Med Res* 2005;**3**(3):166–75.
3. Finn OJ. Cancer immunology. *N Engl J Med* 2008;**358**(25):2704–15.
4. Akira S, Takeda K. Toll-like receptor signalling. *Nat Rev Immunol* 2004;**4**(7):499–511.
5. Melero I, Gaudernack G, Gerritsen W, Huber C, Parmiani G, Scholl S, Thatcher N, Wagstaff J, Zielinski C, Faulkner I, et al. Therapeutic vaccines for cancer: an overview of clinical trials. *Nat Rev Clin Oncol* 2014;**11**(9):509–24.
6. Bergeron A, El-Hage F, Kambouchner M, Lecossier D, Tazi A. Characterisation of dendritic cell subsets in lung cancer micro-environments. *Eur Respir J* 2006;**28**(6):1170–7.
7. Schneider T, Hoffmann H, Dienemann H, Schnabel PA, Enk AH, Ring S, Mahnke K. Non-small cell lung cancer induces an immunosuppressive phenotype of dendritic cells in tumor microenvironment by upregulating B7–H3. *J Thorac Oncol* 2011;**6**(7):1162–8.
8. Melero I, Berman DM, Aznar MA, Korman AJ, Perez Gracia JL, Haanen J. Evolving synergistic combinations of targeted immunotherapies to combat cancer. *Nat Rev Cancer* 2015;**15**(8):457–72.
9. Chen DS, Mellman I. Oncology meets immunology: the cancer-immunity cycle. *Immunity* 2013;**39**(1):1–10.
10. Sabado RL, Balan S, Bhardwaj N. Dendritic cell-based immunotherapy. *Cell Res* 2017;**27**(1):74–95.
11. Yin X, Johns SC, Kim D, Mikulski Z, Salanga CL, Handel TM, Macal M, Zuniga EI, Fuster MM. Lymphatic specific disruption in the fine structure of heparan sulfate inhibits dendritic cell traffic and functional T cell responses in the lymph node. *J Immunol* 2014;**192**(5):2133–42.
12. El Ghazal R, Yin X, Johns SC, Swanson L, Macal M, Ghosh P, Zuniga EI, Fuster MM. Glycan sulfation modulates dendritic cell biology and tumor growth. *Neoplasia* 2016;**18**(5):294–306.
13. Abram CL, Roberge GL, Hu Y, Lowell CA. Comparative analysis of the efficiency and specificity of myeloid-Cre deleting strains using ROSA-EYFP reporter mice. *J Immunol Methods* 2014;**408**:89–100.
14. Schraml BU. Reis e Sousa C: defining dendritic cells. *Curr Opin Immunol* 2015;**32**:13–20.
15. Tkachenko E, Rhodes JM, Simons M. Syndecans: new kids on the signaling block. *Circ Res* 2005;**96**(5):488–500.
16. Thomas JL, Dumouchel J, Li J, Magat J, Balitzer D, Bigby TD. Endotracheal intubation in mice via direct laryngoscopy using an otoscope. *J Vis Exp* 2014(86).
17. Livak KJ, Schmittgen TD. Analysis of relative gene expression data using real-time quantitative PCR and the 2(-Delta Delta C(T)) Method. *Methods* 2001;**25**(4):402–8.
18. Bame KJ, Esko JD. Undersulfated heparan sulfate in a Chinese hamster ovary cell mutant defective in heparan sulfate N-sulfotransferase. *J Biol Chem* 1989;**264**(14):8059–65.
19. Lawrence R, Olson SK, Steele RE, Wang L, Warrior R, Cummings RD, Esko JD. Evolutionary differences in glycosaminoglycan fine structure detected by quantitative glycan reductive isotope labeling. *J Biol Chem* 2008;**283**(48):33674–84.
20. Lawrence R, Kuberan B, Lech M, Beeler DL, Rosenberg RD. Mapping critical biological motifs and biosynthetic pathways of heparan sulfate. *Glycobiology* 2004;**14**(5):467–79.
21. Clausen BE, Burkhardt C, Reith W, Renkawitz R, Forster I. Conditional gene targeting in macrophages and granulocytes using LysMcre mice. *Transgenic Res* 1999;**8**(4):265–77.
22. Savai R, Wolf JC, Greschus S, Eul BG, Schermuly RT, Hanze J, Voswinckel R, Langheinrich AC, Grimminger F, Traupe H, et al. Analysis of tumor vessel supply in Lewis lung carcinoma in mice by fluorescent microsphere distribution and imaging with micro- and flat-panel computed tomography. *Am J Pathol* 2005;**167**(4):937–46.
23. Yin X, Johns SC, Lawrence R, Xu D, Reddi K, Bishop JR, Varner JA, Fuster MM. Lymphatic endothelial heparan sulfate deficiency results in altered growth responses to vascular endothelial growth factor-C (VEGF-C). *J Biol Chem* 2011;**286**(17):14952–62.
24. Rescigno M, Martino M, Sutherland CL, Gold MR, Ricciardi-Castagnoli P. Dendritic cell survival and maturation are regulated by different signaling pathways. *J Exp Med* 1998;**188**(11):2175–80.
25. Chung JS, Dougherty I, Cruz Jr PD, Ariizumi K. Syndecan-4 mediates the coinhibitory function of DC-HIL on T cell activation. *J Immunol* 2007;**179**(9):5778–84.
26. Chung JS, Tamura K, Cruz Jr PD, Ariizumi K. DC-HIL-expressing myelomonocytic cells are critical promoters of melanoma growth. *J Invest Dermatol* 2014;**134**(11):2784–94.
27. Gordts P, Foley EM, Lawrence R, Sinha R, Lameda-Diaz C, Deng L, Nock R, Glass CK, Erbilgin A, Lusis AJ, et al. Reducing macrophage proteoglycan sulfation increases atherosclerosis and obesity through enhanced type I interferon signaling. *Cell Metab* 2014;**20**(5):813–26.
28. Martinez P, Denys A, Delos M, Sikora AS, Carpentier M, Julien S, Pestel J, Allain F. Macrophage polarization alters the expression and sulfation pattern of glycosaminoglycans. *Glycobiology* 2015;**25**(5):502–13.